RSC Advances

PAPER

View Article Online
View Journal | View Issue

Cite this: *RSC Adv.*, 2018, **8**, 42269

Improving the homogeneity of sugarcane bagasse kraft lignin through sequential solvents

Zhuan Jia,[ab] Mingfu Li,[ab] Guangcong Wan,[ab] Bin Luo,[ab] Chenyan Guo,[ab] Shuangfei Wang[ab] and Douyong Min *[ab]

The heterogeneous features of lignin, especially the wide distribution of its molecular weight, limit its high value-added application. To improve the homogeneity of lignin, sugarcane bagasse kraft lignin (KL) dissolved in methanol/acetone (7 : 3, v/v) was successively fractionated into four fractions (*i.e.*., *F*1, *F*2, *F*3, and *F*4) with various organic solvents of decreasing dissolving capacity (*i.e.*., ethyl acetate, ethyl acetate/petroleum ether 1 : 1 v/v, and petroleum ether). The yields of the four fractions (*F*1, *F*2, *F*3, and *F*4) were 59.6, 28.4, 10.8, and 1.2% that of KL, respectively. Gel permeation chromatography (GPC) analysis indicated the molecular weight of each fraction decreased from *F*1 to *F*4. All fractions had a lower polydispersity than KL. KL and the fractions were comprehensively characterized by chemical composition analysis, elemental composition analysis (EA), methoxyl group analysis, Fourier transform infrared spectroscopy (FT-IR), nitrobenzene oxidation analysis (NBO), and nuclear magnetic resonance (NMR) including ^{31}P and ^{1}H–^{13}C HSQC NMR. The results showed that the methoxyl group, hydroxyl group, interunit linkages, and thermal properties of the fractions varied with the molecular weight. The homogeneity of lignin was improved through solvent fractionation.

Received 17th October 2018
Accepted 11th December 2018

DOI: 10.1039/c8ra08595a

rsc.li/rsc-advances

1. Introduction

Lignin is the second renewable natural polymer next to cellulose in the plant world. It is also the only non-petroleum resource that provides renewable aromatic compounds, and it has long been regarded as an excellent raw material for the production of chemicals. Lignin consists of three different types of phenyl-propane units (*p*-hydroxyphenyl (H), syringyl (S), and guaiacyl (G)). These units are linked by a variety of linkages including several types of ethers (*e.g.*, β-O-4, α-O-4) and carbon–carbon linkages (*e.g.*, β–β, β–5). Technical lignin, which is derived from black liquor from papermaking, is primarily incinerated for steam production and power generation. Only a small quantity (<2%)[1] of the lignin worldwide produced is used to produce some high value-added products, such as dispersants,[2,3] adhesives,[4] antioxidants,[5,6] and carbon fiber.[7,8] As people pay more and more attention to environmental issues, lignin has received more and more attention as an environmentally friendly and renewable material. However, the heterogeneous features of technical lignin significantly limit lignin-based applications. According to previous reports,[9,10] the content of lignin functional groups and the thermal stability of lignin are closely related to the molecular weight. Several lignin fractionation methodologies have been used to improve the homogeneity of lignin. To date, four different fractionation methods have been applied including sequential organic solvent extraction,[11,12] selective precipitations at reduced pH values,[13,14] membrane ultrafiltration,[15,16] and ethanol extraction. However, each method has its own limitations, such as expensive organic solvents, the high cost of ultrafiltration, and the recovery of ethanol leading to an increase in cost. Consequently, an economical method for lignin fraction needs to be developed which can improve the homogeneity of lignin effectively.

In this study, based on the solubility and characteristics of lignin in different organic solvents, a process for fractionating KL using inexpensive organic solvents was successfully developed. KL was separated into four fractions by various organic solvents based on their solubility. Eventually, KL and the fractions (*F*1, *F*2, *F*3, and *F*4) were comprehensively characterized by various analytical methods and compared in terms of the yield, molecular weight, content of functional groups, thermal stability, and number of interunit linkages. The results showed that the homogeneity of lignin was increased by solvent fractionation.

2. Material and methods

2.1 Material

The kraft pulping black liquor of sugarcane bagasse was kindly supplied by Guangxi Guitang Co. Ltd. (Guigang, Guangxi, China). All chemicals (AR grade) were purchased from Nanning Lantian Experiment Equipment Company (Nanning, Guangxi, China).

[a]*College of Light Industry and Food Engineering, Guangxi University, Nanning 530004, PR China. E-mail: min.douyong@outlook.com*

[b]*Guangxi Key Laboratory of Clean Pulp & Papermaking and Pollution Control, Nanning 530004, PR China*

2.2 Composition analysis of black liquor

Approximately 5 g of black liquor was dried in an oven at 105 °C for 24 hours to achieve its consistency. The obtained solid was incinerated for 4 h to at 575 °C obtain the black liquor ash content. The quantities of lignin, polysaccharides, and lignin–carbohydrate complex (LCC) in the black liquor were separated and determined according to the reported literature[17] as shown in Fig. 1. Approximately 5 g of black liquor was mixed with 45 mL of deionized water and 100 mL of 1,4-dioxane in a 500 mL beaker, and the pH was adjusted to 2 by 720 μL of sulfuric acid (50 wt%). Then, the mixture was dripped into 450 mL of ethanol/water (95 : 5, v/v) to precipitate the polysaccharide. The polysaccharide was centrifuged and washed with 75 mL of 1,4-dioxane, and the washing liquid was mixed with the previous centrifugate. Then, the polysaccharide was washed with 75 mL of anhydrous ethanol and dried in a vacuum oven at 40 °C for 12 h prior to weighing. The mixture was first subjected to rotary evaporation to remove the ethanol, and then 100 mL of chloroform was added. Finally, extraction separation was carried out in a separatory funnel to obtain an organic layer (1,4-dioxane-chloroform phase) and a precipitation layer. The precipitate layer was dripped into 100 mL of ether to precipitate the LCC. The LCC was then washed twice with ether and dried in a vacuum oven at 40 °C for 12 h prior to weighing; the organic layer was dripped into 200 mL of ether to precipitate lignin. The lignin was washed twice with ether and dried in vacuum at 40 °C for 12 h prior to weighing.

2.3 Lignin extraction

Lignin extraction was carried out according to the following steps. Approximately 5 g of black liquor was first diluted ten times with distilled water and then acidified to pH = 2 with 710 μL of sulfuric acid (50 wt%) to precipitate the lignin. The precipitate was obtained by centrifugation and washed with water until neutral. Subsequently, it was freeze-dried and denoted as sugarcane bagasse kraft lignin (KL).

2.4 Lignin fractionation by sequential organic solvents

KL was sequentially fractionated with the procedure illustrated in Fig. 2. The fractionation started with 5 g of KL dissolved in 17.5 mL of methanol-acetone mixture (7 : 3, v/v). Then the lignin solution was precipitated in 175 mL of ethyl acetate and centrifuged to obtain precipitate I (denoted as *F*1) and centrifugate I. Afterwards, centrifugate I was dripped into 700 mL of ethyl acetate/petroleum ether (1 : 1, v/v) and centrifuged to obtain precipitate II (denoted as *F*2) and centrifugate II. The obtained centrifugate II was first evaporated to 5 mL and precipitated in 50 mL of petroleum ether to obtain precipitate III (denoted as *F*3) and centrifugate III. Centrifugate III was evaporated to obtain the solid (denoted as *F*4).

2.5 Characterizations

2.5.1. Chemical compositions analysis of KL and the fractions. Chemical compositions of KL and the fractions were measured according to the reported method.[18] Briefly, 200 mg lignin was added to 1.5 mL 72% H_2SO_4 in a 25 mL ceramic crucible and the mixture was occasionally stirred for 1.5 h. Then, the mixture was transferred to the conical bottle of 100 mL with 56 mL deionized water and cooked at 120 °C for 2 h. The final solution was filtered into solid and liquor. The collected dried solid was weighed as Klason lignin content. The acid-soluble lignin content in liquor was quantified by UV

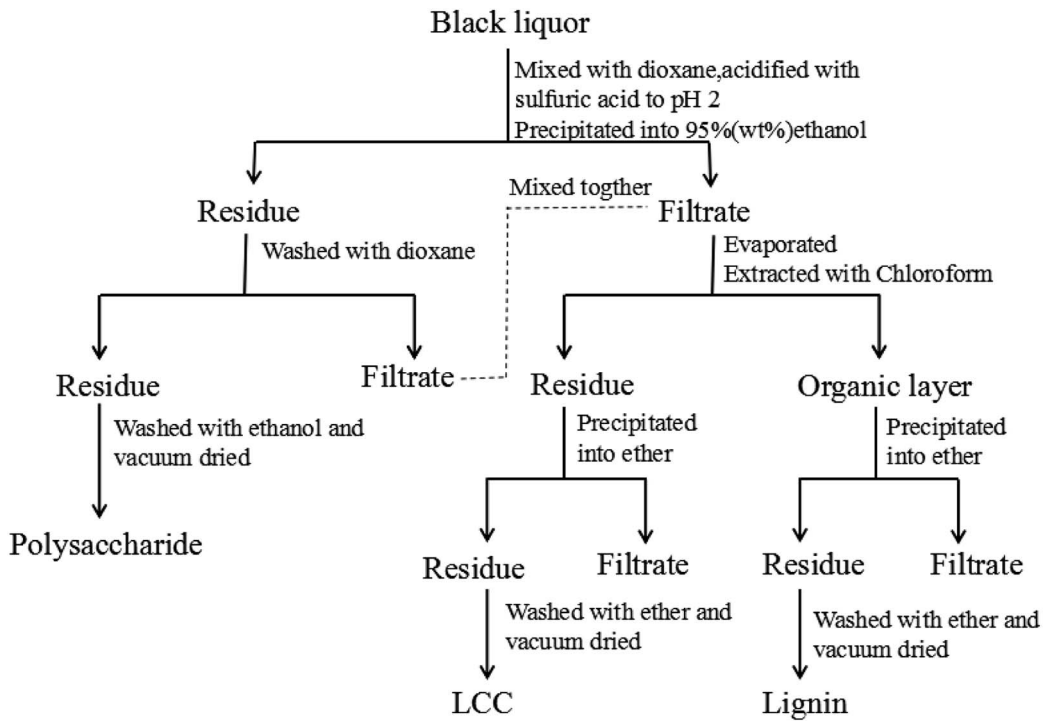

Fig. 1 The schematic procedure for separating lignin, polysaccharide, and LCC from black liquor.

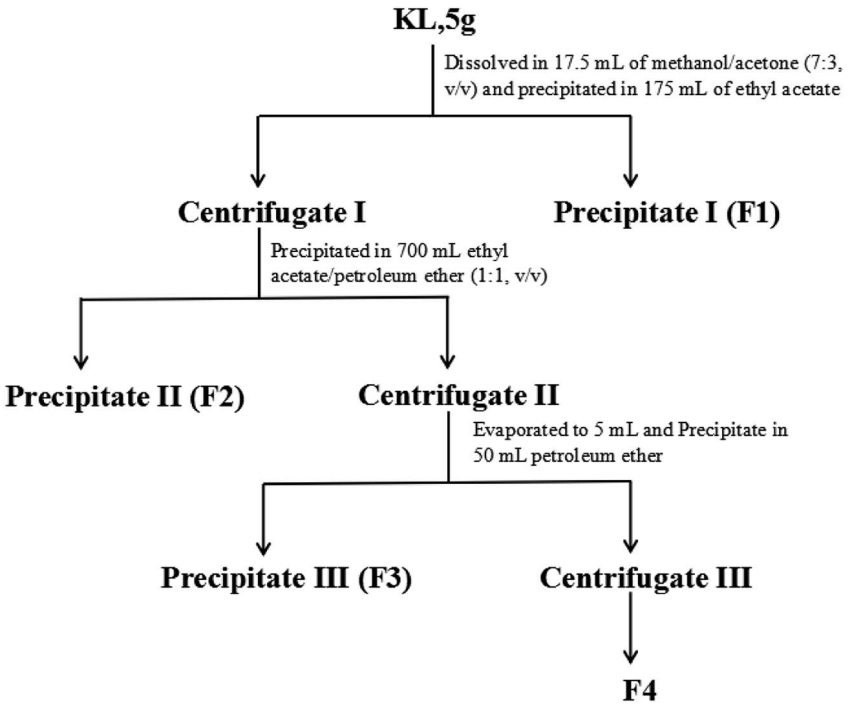

Fig. 2 The schematic fractionation process of kraft lignin.

Table 1 Chemical compositions of KL and the fractions (wt%)

Sample	KL	*F*1	*F*2	*F*3	*F*4
Klason lignin	94.3	89.90	91.05	92.67	93.51
Acid-soluble lignin	3.10	4.70	5.20	2.90	3.80
Total lignin	**97.43**	**94.60**	**96.25**	**95.57**	**97.31**
Arabinan	0.17	0.23	0.14	0.16	0.07
Galactan	0.52	0.71	0.49	0.33	0.21
Glucan	0.09	0.14	0.08	0.10	0.05
Xylan	0.64	0.83	0.69	0.59	0.42
Total sugars	**1.42**	**1.91**	**1.40**	**1.18**	**0.75**
Ash	**0.70**	**0.51**	**0.00**	**0.83**	**0.00**

Table 2 Molecular weights of KL and the fractions

Sample	M_w (g mol^{-1})	M_n (g mol^{-1})	PDI (M_w/M_n)
KL	3242	1077	3.01
*F*1	4205	1442	2.91
*F*2	3239	1200	2.70
*F*3	1951	961	2.03
*F*4	760	522	1.46

spectroscopy at 205 nm. The carbohydrate composition in liquor was determined by IC.[18]

2.5.2. GPC analysis. The acetylation of KL and the fractions was accomplished according to the reported literature.[19] The molecular weights of the acetylated samples were respectively carried out using a 1200 gel permeation chromatograph (Agilent, USA). Tetrahydrofuran was used as the mobile phase. The column temperature was 30 °C, and the flow rate was 0.7 mL min^{-1}. The sample concentration was 1 mg mL^{-1}. And the injection volume was 20 μL. Agilent PL gel MIXED-E column (7.5 × 300 mm, 3 μm) ranging from 500 to 3 × 10^4 was employed. Polystyrene of different molecular weights (mp = 500, 2 × 10^3, 5 × 10^3, 1 × 10^4, and 3 × 10^4 g mol^{-1}, PDI < 1.20) was applied as the sample for the standard carve calibration.

2.5.3. Fourier transform infrared spectrometer analysis (FT-IR). FT-IR analysis of KL and the fractions was respectively performed in a BRUKER TENSOR II instrument (Bruker, Germany). Approximately 1 mg of sample mixed with approximately 200 mg of potassium bromide (KBr) was pressurized to achieve a transparent pallet. Each spectrum was recorded in a frequency range of 800–4000 cm^{-1}. Each sample was scanned 16 times with a resolution of 4 cm^{-1}.

2.5.4. Elemental analysis and methoxyl content determination. Elementary analysis of KL and the fractions was carried out on a PE2400II Elementary Analyzer (PerkinElmer Company, Shanghai, China). The oxygen content of the sample was calculated assuming it only contained C, S, H, N, and O. The methoxyl contents of the samples were determined according to the literature.[20] Briefly, approximately 10.0 mg of sample was reacted with 1 mL of hydroiodic acid (57 wt%) in a headspace test vial (50 mL) at 130 °C for 60 min. After the vial cooled to room temperature, 1 mL of NaOH (6 mol L^{-1}) was injected to neutralize the excess hydroiodic acid. The quantification was carried out in a 6890N gas chromatograph equipped with a G1888 Network Headspace Sampler (Agilent Technologies, California, USA).

2.5.5. Alkaline nitrobenzene oxidation (NBO). The nitrobenzene oxidation process of lignin samples according to the previously method described.[21] Briefly, 10 mg samples, 4 mL

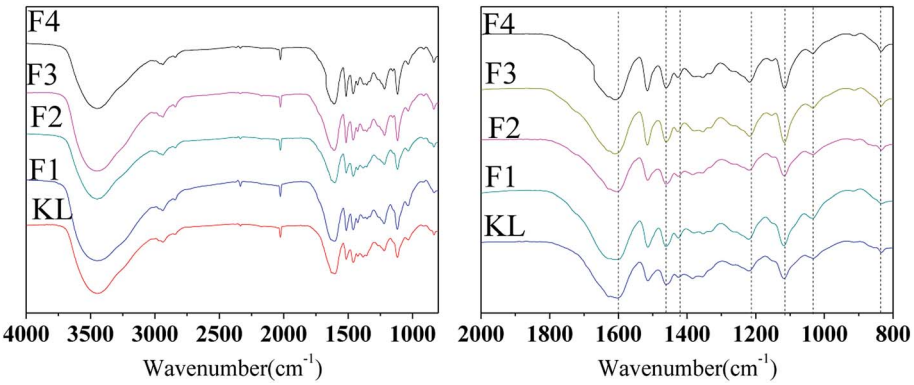

Fig. 3 FT-IR spectra of KL and the fractions.

NaOH (2 mol L^{-1}) solution and 0.25 mL nitrobenzene were added into a stainless-steel bomb reactor with an inner volume of 10 mL Teflon tube, then the reactor was heated to 170 °C for 2 h in an oil bath. After the reaction completed, the reaction tank was quickly placed into the ice water to cool down. And then 1 mL NaOH solution (0.1 mol L^{-1}) containing 0.3 g L^{-1} 3-ethoxy-4-hydroxybenzaldehyde used as an internal standard was added into the resulted mixture. The mixture was acidified to pH 2, and then extracted with dichloromethane (10 mL) three times. The organic layer was dehydrated by anhydrous sodium sulphate, and then it was filtrated and evaporated using a vacuum rotary evaporator at 30 °C to obtain the solid for the derivation. The derivative products were analyzed by GC-MS. The oxidative products were quantified using an Agilent 7890B gas chromatographer (Agilent, American) coupled to an Agilent 5977A mass spectrometer (Agilent Technologies, Palo Alto, CA), and equipped with la HP-5MS UI (30 mm × 0.25 mm × 0.25 mm) column. High-purity helium was used as the carrier gas with a 1 mL min^{-1} flow rate. The initial 40 °C oven temperature was maintained for 3 min, and then given the heating rate of 5 °C min^{-1} go up to 150 °C maintained for 5 min, and then to the heating rate of 5 °C min^{-1} go up to 210 °C maintained for 1 min, finally to given the heating rate of 20 °C min^{-1} go up to 280 °C maintained for 6 min. The total running time was 52.5 min. The inlet temperature was 280 °C, and the split ratio was 1 : 50. The exhaust gas was purged for 4 min, and the injection volume was 1 mL. The spectrometers were operated in the electron-impact (EI) mode, with a 35–350 *m*/*z* scan range. Moreover, the ionization energy was 70 eV and the scan rate was 0.34 s per scan, while the temperature of the ionization source and quadrupole bar was 230 and 150 °C, respectively. The GC-MS data were analyzed using the Agilent ChemStation software.

2.5.6. NMR analysis. NMR analysis of KL and the fractions (*F*1, *F*2, *F*3, and *F*4) was conducted in a Bruker Avance 500 MHz NMR (Bruker, Germany).

^{31}P NMR. ^{31}P NMR spectra were acquired according to methods previously outlined in the literature.[22–24] Briefly, 20 mg of lignin was dissolved in 500 μL of anhydrous pyridine and deuterated chloroform (1.6 : 1, v/v) until completely dissolved. Then, 100 μL of cyclohexanol (10.85 mg mL^{-1}) and 100 μL of chromium(III) acetylacetonate solution (5 mg mL^{-1} in pyridine and deuterated chloroform 1.6 : 1, v/v) were added as an internal standard and relaxation reagent, respectively. Afterwards, 100 μL of phosphitylating reagent (2-chloro-4,4,5,5-tetramethyl-1,3,2-dioxaphosphol) was added to the reaction for 15 minutes under stirring and then it was transferred into an NMR tube. All chemical shifts were correlated to the reaction product of water with 2-chloro-4,4,5,5-tetramethyl-1,3,2-dioxaphosphol, which gave a sharp signal in pyridine/$CDCl_3$ at 132.2 ppm.

^{1}H–^{13}C HSQC. Approximately 150 mg of sample dissolved in 500 μL of dimethyl sulfoxide (DMSO-d_6) was transferred into an NMR tube. The acquisition parameters were as follows: *F*1 spectral width (^{1}H): 19.9947 Hz; scanning number: 16; pulse width selection of P1: 12 μs; acquisition point (TD): 65 536; *F*2 spectral width (^{13}C): 12.9836 Hz; scanning number: 10 000; pulse width of P1: 12 μs; and acquisition point (TD): 1024. The chemical shift was corrected according to the DMSO contour (δ_C/δ_H 39.5/2.5 ppm).

2.5.7. Thermogravimetric analysis (TGA). The thermal stability of KL and the fractions was determined using an STA 449 F5 thermogravimetric apparatus (Netzsch, Germany). Approximately 10 mg of the sample was weighed and placed on a balance in a furnace, and heated at a heating rate of 10 °C min^{-1} under a dry nitrogen atmosphere at a test temperature range of 30 to 800 °C.

Table 3 The assignments of main absorption bands of KL and the fractions[a]

Band (cm^{-1})	Assignments
834	C–H out of plane in G
1031	Aromatic C–H in the plane deformation of G and S
1116	S rings breathing
1164	H rings breathing
1218	C–O stretch vibration
1268	G ring breathing
1329	S skeleton vibration, C–C and C–O stretch vibration
1425	C–H deformation in lignin
1461	Aromatic ring vibration
1514	Aromatic squel vibration
1608	Aromatic squel vibration
1700	C=O stretching in unconjugated or carboxyl groups

[a] S: syringyl; G: guaiacyl.

Table 4 The elemental analysis and the methoxyl content of KL and the fractions

Sample	C (%)	H (%)	O (%)	N (%)	S (%)	OMe (%)	C9 formula	Unit weight
KL	62.0	5.6	31.3	0.6	0.5	14.9	$C_9H_{8.0}O_{2.8}(OCH_3)_{0.92}S_{0.03}$	191
*F*1	53.3	4.8	40.8	0.7	0.4	13.8	$C_9H_{7.8}O_{4.7}(OCH_3)_{1.00}S_{0.03}$	224
*F*2	62.6	5.6	31.0	0.4	0.4	14.7	$C_9H_{7.9}O_{2.8}(OCH3)_{0.89}S_{0.02}$	189
*F*3	63.1	5.8	30.5	0.3	0.3	15.4	$C_9H_{7.8}O_{2.6}(OCH_3)_{0.93}S_{0.02}$	188
*F*4	70.1	8.1	21.3	0.3	0.2	15.9	$C_9H_{8.5}O_{2.5}(OCH_3)_{0.96}S_{0.02}$	186

3. Results and discussion

3.1 Composition of black liquor

The consistency of black liquor was 45%. For the solid part, 19% was ash, 12% was lignin, 8% was polysaccharide, 2% was LCC, and 4% was undefined matter.

3.2 Chemical compositions of lignin

KL was fractionated into four parts (*F*1, *F*2, *F*3, and *F*4) by sequential organic solvent as described in Fig. 2. The yields of the fractions (*F*1, *F*2, *F*3 and *F*4) were 59.6, 28.4, 10.8, and 1.2% that of KL, respectively. The chemical compositions of KL and the fractions are shown in Table 1.

As expected, the lignin contents of KL and the fractions were more than 95%, and only a little amount of residual carbohydrates and ash was identified. The residual carbohydrates in the samples mainly caused from lignin–carbohydrate complex (LCC), in which residual carbohydrates were covalent bonded to lignin, which was little cleaved during kraft pulping process.[25]

3.3 Molecular weight of the samples

The molecular weights and the polydispersity index (PDI) of KL and the fractions are shown in Table 2.

As shown in Table 2, the molecular weights and PDIs of the fractions decreased with the fractionation process. For instance, the M_w of *F*1, *F*2, *F*3, and *F*4 were 4205, 3239, 1951, and 760 g mol^{-1}, respectively. The PDIs of *F*1, *F*2, *F*3, and *F*4 were 2.91, 2.70, 2.03, and 1.46, respectively. It was reported by Wang and Chen[26] that the solubility of lignin was related to its molecular weight. The lignin with higher molecular weight more preferred to remain in the solid part, which was consistent with our result. As a mixture of the fractions, KL possessed a lower molecular weight (M_w is 3242 g mol^{-1}) compared to *F*1 (M_w is 4205 g mol^{-1}) but a higher PDI (3.01), which was explained by the cleavages of the interunit linkages of lignin during the kraft pulping process. A similar result was reported previously.[20] The GPC analysis indicated that the organic solvent fractionation can effectively improve the homogeneity of lignin.

3.4 FT-IR analysis

The FT-IR spectra of KL and the fractions are demonstrated in Fig. 3. The main bands assigned according to the literature[24] are summarized in Table 3.

The peaks at 834 and 1268 and 1116 and 1329 cm^{-1} were assigned to guaiacyl (G) and syringyl (S), respectively. Moreover, the peak at 1166 cm^{-1} was assigned to *p*-hydroxyl phenyl propane (H) unit according to the literature,[27] indicating that the bagasse lignin was normally HGS type lignin. The presence of G-type unit indicated that sugarcane bagasse lignin possessed potential active sites for polymerization. For instance, phenol condenses initially with formaldehyde in the presence of alkaline to form methylolphenol during phenol formaldehyde condensation reactions.[28] Few structural differences between KL and the fractions indicated that the organic solvents fractionation hardly altered the lignin structure and only improved the homogeneity of lignin. In accordance with previous reports, the typical peaks of lignin fractions and the starting lignin were closely similar but different in intensity.[20,26]

3.5 Elemental and methoxyl content analyses

The C9 formula and the molecular weights of KL and the fractions were calculated by elemental analysis and methoxyl content determination, as shown in Table 4.

The sulfur element remained in each fraction, even though the starting KL had been thoroughly washed before the fractionation. The sulfur element identified in lignin may be derived from hydrosulfide anions during the kraft pulping process. It was previously reported[29] that kraft lignin contains 29% inorganic, 1% elemental, and 70% organically bonded sulfur. The sulfur remaining in the fractions was the organically bonded sulfur according to the reported literature.[18] The nitrogen content was potentially due to the formation of protein-lignin complexes during the delignification process.[30] The methoxyl contents increased from *F*1 to *F*4 (weight percent), whereas *F*4 possessed the highest methoxyl content which is 15.9% indicating that the syringyl lignin was more easily

Table 5 Yields of the oxidative products of KL and the fractions (wt%)[a]

Oxidative products	KL	*F*1	*F*2	*F*3	*F*4	Pine KL[18]
Syringaldehyde	12.2	4.2	10.0	15.5	4.1	N.D.
Syringic acid	6.3	7.0	8.0	3.9	1.3	N.D.
4-Hydroxybenzaldehyde	1.8	1.8	0.8	1.8	13.4	0.4
4-Hydroxybenzoic acid	1.2	2.2	2.8	0.9	3.1	N.D.
Vanillin	5.7	8.5	3.2	4.0	8.1	4.3
Vanillic acid	N.D.	N.D.	N.D.	N.D.	0.4	17.3
Total	27.2	23.7	24.8	26.1	29.9	22.0

[a] N.D. stands for not detected.

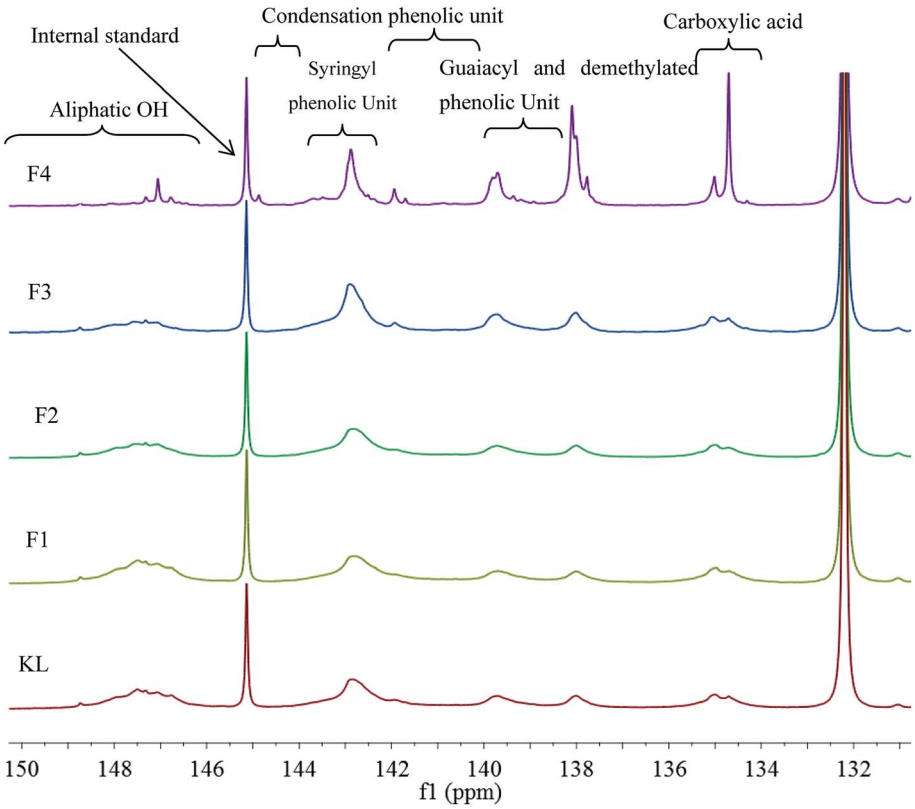

Fig. 4 ^{31}P NMR spectra of KL and the fractions.

fragmented and dissolved in the pulping black liquor during the kraft pulping process. A similar result had been reported.[31]

3.6 Alkaline nitrobenzene oxidation

The basic structural information of lignin was achieved by alkaline nitrobenzene oxidation. Based on the yield of the oxidative products (phenolic aldehydes and corresponding acids) of lignin, the condensation degree of lignin was obtained because only non-condensed parts of lignin were oxidized by alkaline nitrobenzene oxidation. And the ratio of syringyl aldehyde to vanillin (S/V) was calculated from the corresponding oxidative products. The yield of the oxidative products from KL and the fractions were summarized in Table 5.

It was showed in Table 5 that the total yield of oxidative products of KL was 27.2%, whereas that of fraction *F*1, fraction *F*2, fraction *F*3, and fraction *F*4 was respectively 23.7, 24.8, 26.1, and 29.9%. Thus, *F*1 had the highest degree of condensation while the fraction *F*4 had the least degree of condensation according to the yield of the oxidative products. Compared to pine KL used as a reference, both of yields of the oxidative products of KL and the fractions were higher than that of pine-KL.[18] It was proposed that the pine lignin is enriching of G-type lignin and G-type lignin was more preferred than S-type lignin to condense during kraft pulping process. The existence of three aldehydes (syringaldehyde, 4-hydroxybenzaldehyde, and vanillin) and the corresponding acids (syringic acid, 4-hydroxybenzaldehyde, and vanillic acid) indicates that the lignin structure in bagasse was a typical HGS type, which is consistent to the result of FT-IR analysis.

3.7 ^{31}P NMR analysis

The hydroxyl group, *i.e.*, alcoholic hydroxyl and phenolic hydroxyl, is one of the most important functional groups of lignin, which is also the main active site for the chemical modification of lignin. Therefore, the hydroxyl content was an important part of the lignin molecular structure analysis. The ^{31}P NMR spectra of KL and the fractions are shown in Fig. 4, and the quantitative results are listed in Table 6.

Table 6 indicates that the total phenolic hydroxyl content was correlated to the molecular weight of the sample. For

Table 6 The contents of the hydroxyl groups (mmol g^{-1}) quantified by ^{31}P NMR

		Lignin samples (mmol g^{-1})				
Assignment	δ	KL	*F*1	*F*2	*F*3	*F*4
Aliphatic OH	146.3–150.8	0.71	0.92	0.44	0.28	0.27
Condensed phenolic OH	144.3–140.2	1.41	1.27	1.58	1.93	1.48
Syringyl OH (S)	143.7–142.2	1.23	1.02	1.37	1.73	1.13
Guaiacyl OH	140.2–138.4	0.35	0.33	0.37	0.53	0.80
Catechol	139.0–138.2	0.02	0.04	0.03	0.06	0.20
p-Hydroxy phenyl (H) OH	138.6–136.9	0.15	0.14	0.16	0.38	1.35
Carboxylic acid	135.6–133.7	0.38	0.38	0.34	0.45	1.00
Total phenolic OH	—	1.91	1.74	2.11	2.85	3.63

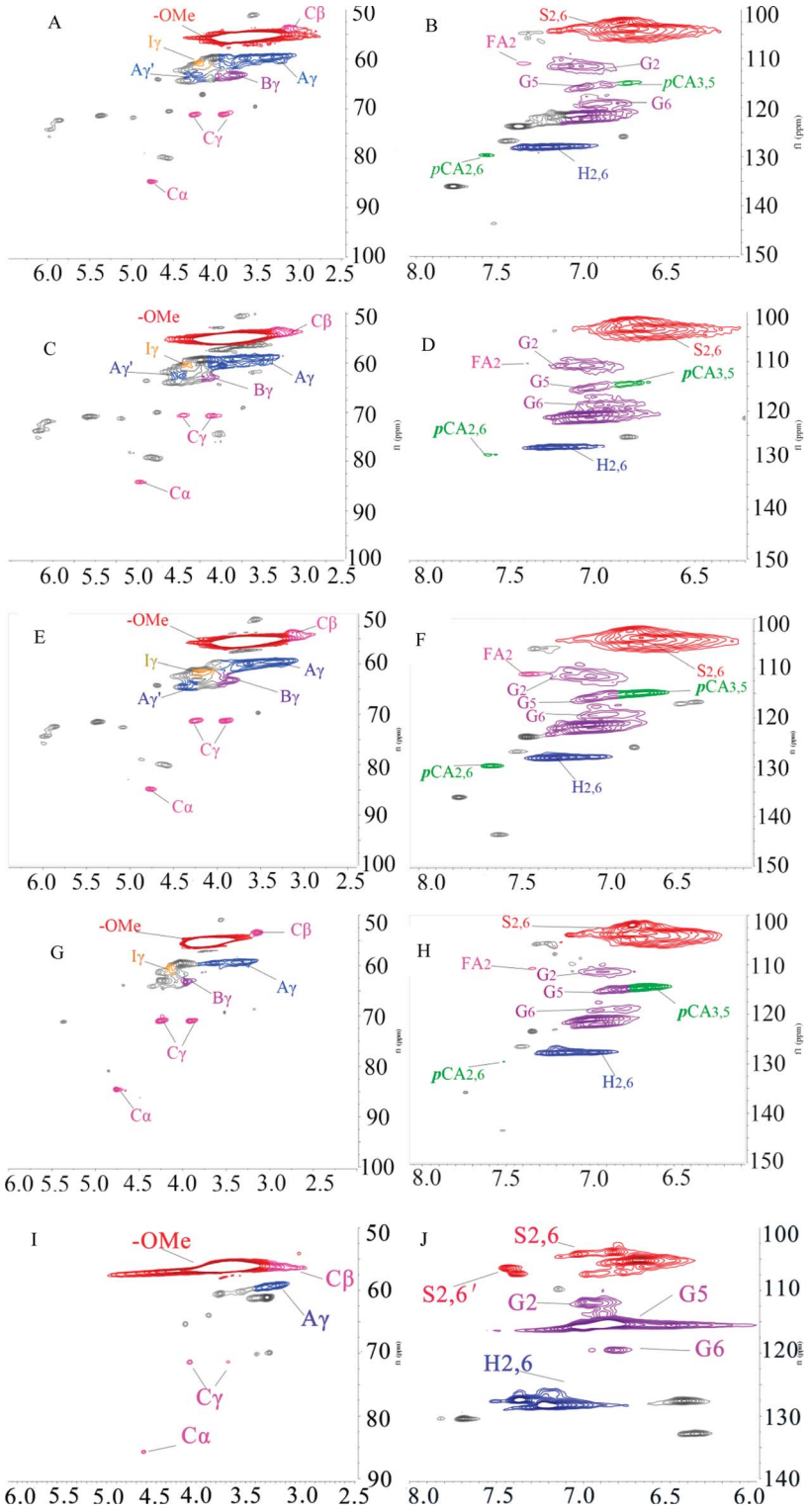

Fig. 5 2D HSQC NMR spectra of KL and the fractions, (A) side chain region of KL; (B) aromatic region of KL; (C) side chain region of *F*1; (D) aromatic region of *F*1; (E) side chain region of *F*2; (F) aromatic region of *F*2; (G) side chain region of *F*3; (H) aromatic region of *F*3; (I) side chain region of *F*4; (J) aromatic region of *F*4.

example, the total phenolic hydroxyl content of KL was only 1.91 mmol g^{-1}; however, the total phenolic hydroxyl content of *F*4 was increased to 3.63 mmol g^{-1}, which corresponded to the cleavages of aryl ether bond (β-O-4) of lignin during the kraft pulping process. The cleavage of β-O-4 induced lignin fragmentation and its solubilization in black liquor, and the generation of new phenolic hydroxyl on the lignin fragments.[19] The aliphatic hydroxyl content also correlated to the molecular

weight of the sample. For instance, the aliphatic hydroxyl content of KL was 0.71 mmol g^{-1}; however, that of *F*4 was decreased to 0.27 mmol g^{-1}, which was explained by the removal of α- or γ-hydroxyl on the side chain through the formation of methylene quinone intermediate during the kraft process. Similar results have been previously reported.[12,32] In addition, the catechol content increased from *F*1 to *F*4. For example, the catechol of *F*1 was only 0.02 mmol g^{-1}. Nonetheless, that of *F*4 increased to 0.2 mmol g^{-1} can be explained by the demethylation of lignin during the kraft pulping process.[33]

3.8 2D HSQC NMR analyses

^{1}H–^{13}C HSQC NMR was used to characterize the lignin structure. The 2D HSQC NMR spectrum can be defined as two main regions: the side chain region (δ_C/δ_H 50–90/2.5–6.5 ppm) and the aromatic region (δ_C/δ_H 100–140/5.5–8.0 ppm), as shown in Fig. 5. The HSQC spectra and main substructures of lignin identified by 2D HSQC NMR are shown in Fig. 5 and 6. The main contours were assigned according to the literature and are summarized in Table 7.[34,35]

The peaks at δ_C/δ_H 60.0/3.43 ppm and δ_C/δ_H 63.1/4.36 ppm were assigned to C_γ of aryl ether (β-O-4 structure) (denoted as A_γ) and C_γ–OH of alkyl-aryl ethers (β-O-4) acylated with *p*CA, respectively (shown in Fig. 5). The peak at δ_C/δ_H 56.2/3.73 ppm was assigned to the methoxyl group. Due to its stability during the kraft pulping process, the methoxyl group content was set as the internal standard for the quantitative analysis of interunit linkages of lignin. The peaks at δ_C/δ_H 111.0/7.02 ppm, δ_C/δ_H 115.1/6.72 ppm, and δ_C/δ_H 119.0/6.77 ppm were respectively assigned to G_2, G_5, and G_6. The peak at δ_C/δ_H 103.8/6.69 ppm was assigned to $S_{2/6}$. The peak at δ_C/δ_H 128.0/7.23 ppm was assigned to $H_{2/6}$. The presence of G-units, H-units, and S-units indicated that sugarcane bagasse lignin is HSG-type lignin which was consistent with the FT-IR analysis. The small signals assigned to FA and *p*CA were identified (in Fig. 5) because most of the hydroxycinnamic acids were removed during the kraft pulping process.[36]

The main interunit linkages of the samples were quantified according to the literature,[18] and the results are summarized in Table 8. KL had a higher content of condensed linkages, *i.e.*, β–β′ linkages (5.0/100C9) and β–5′ (0.6/100C9) and a lower content of noncondensed linkages, *i.e.*, β-O-4′ (1.3/100C9). It has been suggested that the cleavage of aryl ether bonds (β-O-4′) induced the fragmentation of lignin, and the condensation of the generated lignin fragments occurred during the kraft pulping process.[35] Table 8 shows that the fractions had different structures. Compared to KL, *F*1 and *F*2 had lower condensed linkages (β–5′ and β–β′) but higher noncondensed linkages (β-O-4′). However, *F*3 and *F*4 had higher condensed linkages but lower noncondensed linkages which was consistent with the reported result.[20] Compared to aryl ether bond (β-O-4′), the C–C bonds (β–5′ and β–β′) were more stable during the kraft pulping process. Thus, the fragmentation of lignin was induced by the cleavages of β-O-4′ which reduced the molecular weight and increased the phenolic hydroxyl group content of lignin. Consequently, the fraction with a lower molecular weight had

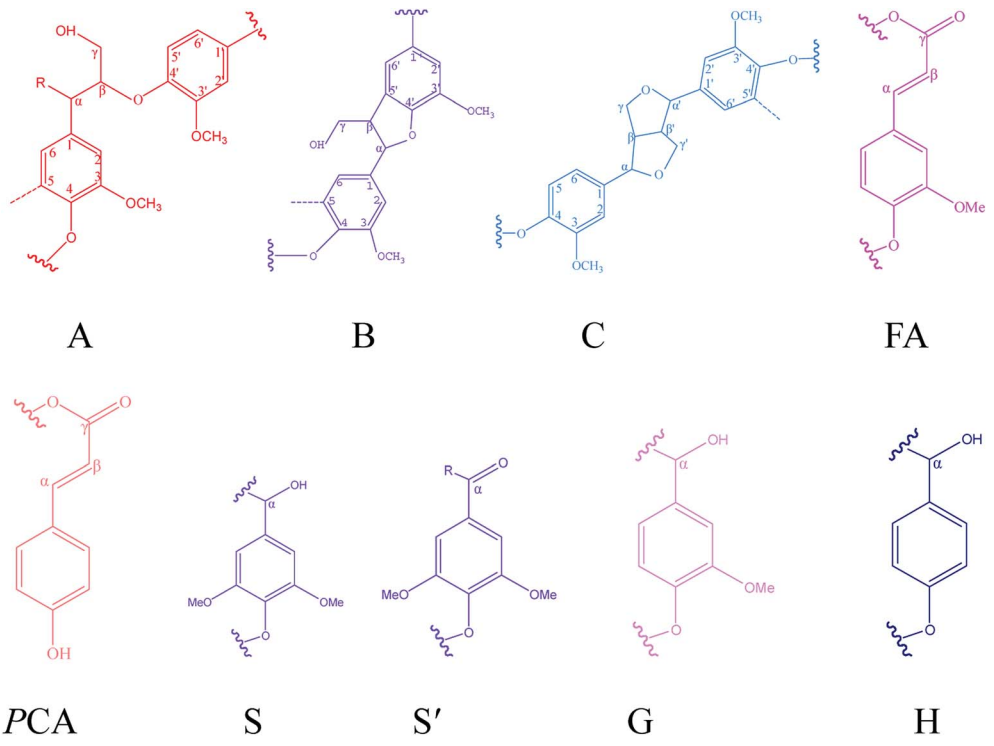

Fig. 6 Main interunit linkages and aromatic units of KL and the fractions identified by HSQC, A: β-O-4′ linkages; B: β–5′ linkages; C: β–β′ linkages; FA: ferulates; *p*CA: *p*-coumarates; S: syringyl units; S′: C_α-oxidized syringyl unit; G: guaiacyl unit; H: *p*-hydroxyphenyl unit.

Table 7 The assignments of the main interunit linkages of KL and the fractions

Label	δ_C/δ_H	Assignment
B_β	53.3/3.48	C_β–H_β in β–5′ substructures (B)
C_β	53.5/3.08	C_β–H_β in pinoresinol substructures (C)
A_γ	60.0/3.43	C_γ–H_γ in β-O-4′ substructures (A)
I_γ	61.3/4.13	C_γ–H_γ in coniferyl alcohol end groups (I)
B_γ	62.7/3.70	C_γ–H_γ in β–5′ substructures (B)
C_γ	70.7/3.76 and 4.17	C_γ–H_γ in pinoresinol substructures (C)
C_α	84.8/4.63	C_α–H_α in pinoresinol substructures (C)
$S'_{2,6}$	106.4/7.31	$C_{2,6}$–$H_{2,6}$ in oxidized (C_α=O) syringyl units (S′)
$S_{2,6}$	103.8/6.69	$C_{2,6}$–$H_{2,6}$ in syringyl units (S)
G_2	111.0/7.02	C_2–H_2 in guaiacyl units (G)
G_5	115.1/6.72	C_5–H_5 in guaiacyl units (G)
G_6	119.0/6.77	C_6–H_6 in guaiacyl units (G)
$H_{2,6}$	127.9/7.01	$C_{2,6}$–$H_{2,6}$ in *p*-hydroxyphenyl units (H)
$pCA_{2,6}$	130.0/7.50	$C_{2,6}$–$H_{2,6}$ in free *p*-coumaric acid (*p*CA)
pCA_α/FA_α	144.1/7.50	C_α–H_α in free *p*-coumaric acid (*p*CA) and ferulic (FA) acids
$pCA_{3,5}$	115.5/6.79	*p*-Coumarate
FA_2	110.9/7.32	Ferulate
FA_6	122.5/7.15	Ferulate

Table 8 Quantitative analysis of the main interunit linkages of KL and the fractions[a]

Linkage	KL	*F*1	*F*2	*F*3	*F*4	Pine KL[18]
β-O-4	1.3	1.5	1.2	0.9	0.3	2.2
β–5′	0.6	0.8	0.5	0.4	N.D.	1.6
β–β′	5.0	4.8	4.2	5.4	5.6	6.0

[a] All values are based on 100C9; N.D.: not detectable.

higher contents of phenolic hydroxyl group and condensed linkages. For example, the total phenolic hydroxyl group of *F*4 was 3.63 mmol g^{-1} (shown in Table 6), and the condensed linkages of *F*4 were 5.6/100C9 (shown in Table 8). Compared to pine KL as a reference,[18] the content of β–5′ was higher than that of sugarcane bagasse lignin. Pine lignin is more enriched of G-type unit than sugarcane bagasse lignin which induced the more of β–5′ linkages in original lignin. Besides G-type lignin possessed more open C5 position which was more prone to condense for new formatting of β–5′ during kraft pulping process.

3.9 Thermal analyses

The thermodynamic properties of lignin are important factors affecting its thermochemical conversion to chemicals, energy, or materials. The TGA analysis of KL and the fractions is shown in Fig. 7 and Table 9.

Table 9 indicates that the "coke residue" of KL, *F*1, *F*2, *F*3, and *F*4 at 800 °C was 42.7, 40.1, 40.1, 34.4, and 13.6%, respectively. Fractions *F*1 and *F*2 with the highest residual coke yields may be more valuable than the other fractions in the production of activated carbon or carbon fiber with lignin as the carbon precursor.[31] The decomposition curves of KL and the fractions were different, which indicated the heterogeneity of the kraft lignin. The maximum decomposition temperatures (T_M) of KL, *F*1, *F*2, *F*3, and *F*4 were respectively 377, 372, 386, 389, and 209 °C. According to previous reports, the lignin with higher the molecular weight possessed better the thermal stability.[9,37] The fraction of *F*4 with the lowest molecular weight possessing the smallest T_M was expected, while the increase in the T_M of *F*1, *F*2 and *F*3 with decreasing molecular weight was unexpected. This was explained by that the thermal stability of lignin was not only affected by its molecular weight.[29] It was found that the T_M of

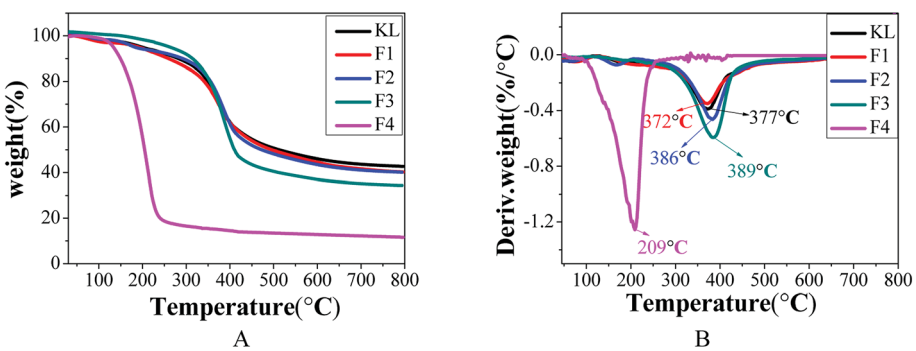

Fig. 7 TGA analysis of KL and the fractions, (A) TG curves; (B) DTG curves.

Table 9 T_M and residue char of KL and the fractions

Lignin sample	T_M/°C	PDI/M_w/M_n	Residue char/%
KL	377	3.01	42.7
*F*1	372	2.91	40.1
*F*2	386	2.70	40.1
*F*3	389	2.03	34.4
*F*4	209	1.46	13.6

the fractions (*F*1, *F*2, and *F*3) shifted to higher temperatures with reduced polydispersity. The T_M of *F*4 possessed the minimum of 209 °C, although *F*4 had the lowest polydispersity (PDI = 1.46). However, this was explained by the fact that the molecular weight of *F*4 was extremely small (M_w = 760).[35] In conclusion, the thermal stability of lignin was related not only to its molecular weight but also to its polydispersity.

4. Conclusions

Sugarcane bagasse KL was separated into four fractions (*F*1, *F*2, *F*3, and *F*4) by sequential solvent fractionation. Afterwards, KL and the fractions were comprehensively characterized by wet chemistry and spectroscopies. The homogeneity of lignin was improved effectively by the sequential solvent fractionation because the fractions possessed specific solubility in different solvents. Compared to KL and *F*1, *F*2, and *F*3, fraction *F*4 had a relatively lower molecular weight and possessed more methoxyl groups, phenolic hydroxyl groups, and catechol. The thermal properties of lignin were affected by the combination of molecular weight and polydispersity. NBO analysis indicated that *F*4 possessed the lowest degree of condensation. *F*1, *F*2, and *F*3, T_M increased with the decrease in polydispersity. However, *F*4 possessed the lowest T_M but the lowest polydispersity, which can be explained by its lowest molecular weight.

Conflicts of interest

There are no conflicts to declare.

Acknowledgements

This research was financially supported by the Natural Science Foundation of China (NSFC No. 31400514), Postdoctoral Science Foundation of China (No. 2015M570419), the Foundation of State Key Laboratory of Pulp and Paper Engineering (2015016), and the Foundation of Guangxi Key Laboratory of Clean Pulp & Papermaking and Pollution Control (ZR201805-7).

References

1 H. J. Huang, S. Ramaswamy, U. W. Tschirner and B. V. Ramarao, *Sep. Purif. Technol.*, 2008, **62**, 1–21.
2 H. R. Wu, F. G. Chen, Q. H. Feng and X. P. Yue, *BioResources*, 2012, **7**, 2742–2751.
3 W. M. He, W. J. Gao and P. Fatehi, *ACS Sustainable Chem. Eng.*, 2017, **5**, 10597–10605.
4 N. Tachon, B. Benjelloun-Mlayah and M. Delmas, *BioResources*, 2016, **11**, 5797–5815.
5 R. Kaur, S. K. Uppal and P. Sharma, *Sugar Tech*, 2017, **19**, 675–680.
6 M. D. Garrison and B. G. Harvey, *J. Appl. Polym. Sci.*, 2016, **133**, 1–12.
7 J. Lin, T. Yamada, K. Koda and Y. Uraki, *BioResources*, 2012, **7**, 5634–5646.
8 L. Salmén, E. Bergnor, A. M. Olsson, M. Akerstrom and A. Uhlin, *BioResources*, 2015, **10**, 7544–7554.
9 H. Hatakeyama and T. Hatakeyama, *Adv. Polym. Sci.*, 2009, **232**, 1–63.
10 Y. Hirohisa, M. Roland and K. P. Kringstad, *Holzforschung*, 1987, **41**, 171–176.
11 M. F. Li, S. N. Sun, F. Xu and R. C. Sun, *Sep. Purif. Technol.*, 2012, **101**, 18–25.
12 C. Z. Cui, R. K. Sun and D. S. Argyropoulos, *ACS Sustainable Chem. Eng.*, 2014, **2**, 959–968.
13 P. S. B. dos Santos, X. Erdocia, D. A. Gatto and J. Labidi, *Ind. Crops Prod.*, 2014, **55**, 149–154.
14 G. H. Wang and H. Z. Chen, *Sep. Purif. Technol.*, 2013, **105**, 98–105.
15 A. Toledano, A. Garcia, I. Mondragon and J. Labidi, *Sep. Purif. Technol.*, 2010, **71**, 38–43.
16 A. S. Jönsson, A. K. Nordin and O. Wallberg, *Chem. Eng. Res. Des.*, 2008, **86**, 1271–1280.
17 T. Dai, S. B. Wu and D. L. Guo, *J. Fuel Chem. Technol.*, 2013, **41**, 169–176.
18 Z. J. Hu, X. Y. Du, J. Liu, H. M. Chang and H. Jameel, *J. Wood Chem. Technol.*, 2016, **36**, 432–446.
19 W. G. Glasser, V. Dave and C. E. Frazier, *J. Wood Chem. Technol.*, 1993, **13**, 545–559.
20 H. L. Li, X. S. Chai, M. R. Liu and Y. H. Deng, *J. Agric. Food Chem.*, 2012, **60**, 5307–5310.
21 L. F. Yang, MPhil, Nanjing Forestry University, 2013.
22 A. Granata and D. S. Argyropoulos, *J. Agric. Food Chem.*, 1995, **43**, 1538–1544.
23 D. S. Argyropoulos, *J. Wood Chem. Technol.*, 1994, **14**, 45–63.
24 A. Guerra, I. Filpponen, L. A. Lucia, C. Saquing, S. Baumberger and D. S. Argyropoulos, *J. Agric. Food Chem.*, 2006, **54**, 5939–5947.
25 T. M. Liitia, S. L. Maunu, B. Hortling, M. Toikka and I. Kilpelainen, *J. Agric. Food Chem.*, 2003, **51**, 2136–2143.
26 G. Wang and H. Chen, *Sep. Purif. Technol.*, 2013a, **120**, 402–409.
27 N. Shukry, S. M. Fadel, F. A. Agblevor and S. F. EI-Kalyoubi, *J. Appl. Polym. Sci.*, 2008, **109**, 434–444.
28 X. B. Zhao, L. M. Dai and D. H. Liu, *J. Appl. Polym. Sci.*, 2009, **114**, 1295–1302.
29 A. Moubarik, N. Grimi, N. Boussetta and A. Pizzi, *Ind. Crops Prod.*, 2013, **45**, 296–302.
30 R. Mörck, H. Yoshida, K. P. Kringstad and H. Hatakeyama, *Holzforschung*, 1986, **40**, 51–60.
31 X. Jiang, D. Savithri, X. Y. Du, S. Pawar, H. Jameel, H. M. Chang and X. F. Zhou, *ACS Sustainable Chem. Eng.*, 2017, **5**, 835–842.

32 X. B. Zhao, L. M. Dai and D. H. Liu, *J. Appl. Polym. Sci.*, 2009, **114**, 1295–1302.
33 I. Brodin, E. Sjöholm and G. Gellerstedt, *Holzforschung*, 2009, **63**, 290–297.
34 A. T. Martínez, J. Rencoret, G. Marques, A. Gutierrez, D. Ibarra, J. Jimenez-Barbero and J. C. del Rio, *Phytochemistry*, 2008, **69**, 2831–2843.
35 J. Rencoret, G. Marques, A. Martínez, L. Nieto, J. Jimenez-Barbero and J. C. del Rio, *Ind. Crops Prod.*, 2009, **30**, 137–143.
36 F. Xu, R. C. Sun, J. X. Sun, C. F. Liu, B. H. He and J. S. Fan, *Anal. Chim. Acta*, 2005, **552**, 207–217.
37 X. J. Shen, B. Wang, P. L. Huang, J. L. Wen and R. C. Sun, *Rsc. Adv.*, 2016, **6**, 45315–45325.